

THE *WISE* LIGHT CURVES OF Z CAMELOPARDALIS DURING OUTBURST: EVIDENCE FOR SYNCHROTRON EMISSION?

THOMAS E. HARRISON

Department of Astronomy, New Mexico State University, P.O. Box 30001, MSC 4500, Las Cruces, NM 88003-8001, USA; tharriso@nmsu.edu
Received 2014 May 29; accepted 2014 July 17; published 2014 July 28

ABSTRACT

The *WISE* mission happened to observe the cataclysmic variable Z Cam at the peak of an outburst. The *WISE* single exposure data shows that Z Cam was highly variable at $12\ \mu\text{m}$, but only marginally so at shorter wavelengths. The rapid variability at $12\ \mu\text{m}$, and the fact that these observations occurred close to visual maximum suggests that, like SS Cyg, Z Cam is a synchrotron source.

Key words: infrared: stars – novae, cataclysmic variables – stars: individual (Z Cam)

1. INTRODUCTION

Z Cam is the prototype of a small subgroup of the cataclysmic variables (CVs) that show “standstills” in their light curves where the system can persist in a state of relatively constant brightness that is well above minimum light, but can be a magnitude or more below that attained in a normal outburst. There are about 20 confirmed members of this class (Simonsen et al. 2014). In the thermal-viscous “disk instability model” (DIM) interpretation for the behavior of dwarf novae (see Cannizzo et al. 2010 and references therein), it is believed that Z Cam stars are accreting at a rate that is close to the transition point between the hot, stable accretion disks of the high mass transfer rate nova-like variables, and the unstable, lower mass accretion rate dwarf novae (Honeycutt et al. 1998; Shafter et al. 2005). Additional support for this interpretation is that Z Cam stars typically have short recurrence times between outbursts given their relatively long orbital periods ($P_{\text{orb}} \geq 3$ hr; Warner 1995). This suggests a more rapid replenishing of the accretion disk following an outburst.

One of the more interesting discoveries about CVs in the past decade was the detection of synchrotron emission from SS Cyg during outburst (Körding et al. 2008). While synchrotron emission from the peculiar, highly magnetic CV system AE Aqr has been known for a while (Bastian et al. 1988), there had remained an open question as to whether non-magnetic CVs were capable of spawning synchrotron jets (Livio 1999; Soker & Lasota 2004). In constructing a pseudo-hardness/intensity diagram for SS Cyg, Körding et al. analogize the behavior of SS Cyg with the jet-launching realms observed in X-ray binaries. Harrison et al. (2010) concluded that the mysterious *IRAS* detection of SS Cyg (Jameson et al. 1987) was in fact due to the detection of its transient synchrotron jet. Thus, like in many X-ray binaries (see Harrison et al. 2014 and references therein), the synchrotron emission from SS Cyg extends into the mid-infrared (mid-IR). Dubus et al. (2004) observed that SS Cyg was highly variable in quiescence at 4.8 and $11.7\ \mu\text{m}$. They suggested that this variability might be accounted for by free-free emission in a wind, though the derived mass loss rate was very high, similar to the system’s accretion rate. Perhaps the variability of SS Cyg in quiescence can also be tied to synchrotron processes.

In a survey of *WISE* data for CVs that we have undertaken, we were struck by the brightness of Z Cam—it was the third brightest dwarf nova in the $12\ \mu\text{m}$ bandpass. Upon further

investigation, we found that the *WISE* observations of Z Cam were obtained during the peak of a normal outburst. As we describe below, the mid-IR light curves of Z Cam suggest that it is a likely synchrotron source. In the next section we present the data sets for Z Cam, in Section 3 we discuss those data, and in Section 4 we draw our conclusions.

2. THE MID-INFRARED OBSERVATIONS OF Z CAM

The *WISE* mission (Wright et al. 2010) surveyed the entire sky in four wavelength bands: 3.4 , 4.6 , 12 , and $22\ \mu\text{m}$. The two short bandpasses (“W1” and “W2”) are similar to the two short *Spitzer* IRAC bandpasses. The $12\ \mu\text{m}$ channel (“W3,” $\lambda_{\text{eff}} = 11.56\ \mu\text{m}$), is similar to that of the *IRAS* $12\ \mu\text{m}$ bandpass, while the $22\ \mu\text{m}$ (“W4”; $\lambda_{\text{eff}} = 22.09\ \mu\text{m}$) bandpass closely resembles the *Spitzer* MIPS $24\ \mu\text{m}$ channel (Jarrett et al. 2011). Due to the scanning nature of its orbit, every object was observed by *WISE* on at least 12 separate occasions. Thus, it is possible to generate light curves using the “single exposure” observations from the *WISE* mission. We have extracted both the light curve data, as well as the “AllWISE” point source fluxes for Z Cam using the IRSA Web site (<http://irsa.ipac.caltech.edu/>). The point source catalog fluxes for Z Cam are listed in Table 1.

Unlike the magnitudes presented in the AllWISE point source catalog, the single exposure source light curves can have defects due to a number of effects.¹ In addition, there are slight offsets between the mean magnitudes derived from the single exposure data, and the final AllWISE point source catalog fluxes due to enhancements in the calibration of the individual light curve data used in the latter. We present the *WISE* light curves of Z Cam in Figure 1. In the bottom panel, we present the light curves of the brightest nearby source, J082423.40+730628.9, to confirm that the light curve variations seen in Z Cam are not due to spurious effects. Note that the single exposure observation at MJD55287.160436 is deviant in both the nearby star and in Z Cam. Outside of this single observation, the field star light curves suggest that (at its brightness) the standard deviations in the three light curves are $\sigma = \pm 0.05$, 0.04 , and 0.14 mag, respectively. Obviously, the field star is substantially fainter than Z Cam in the W3 band, and thus its light curve in this bandpass is considerably noisier. However, this source remains constant to within the W3 error bars.

¹ See http://wise2.ipac.caltech.edu/docs/release/allsky/expsup/sec4_4a.html.

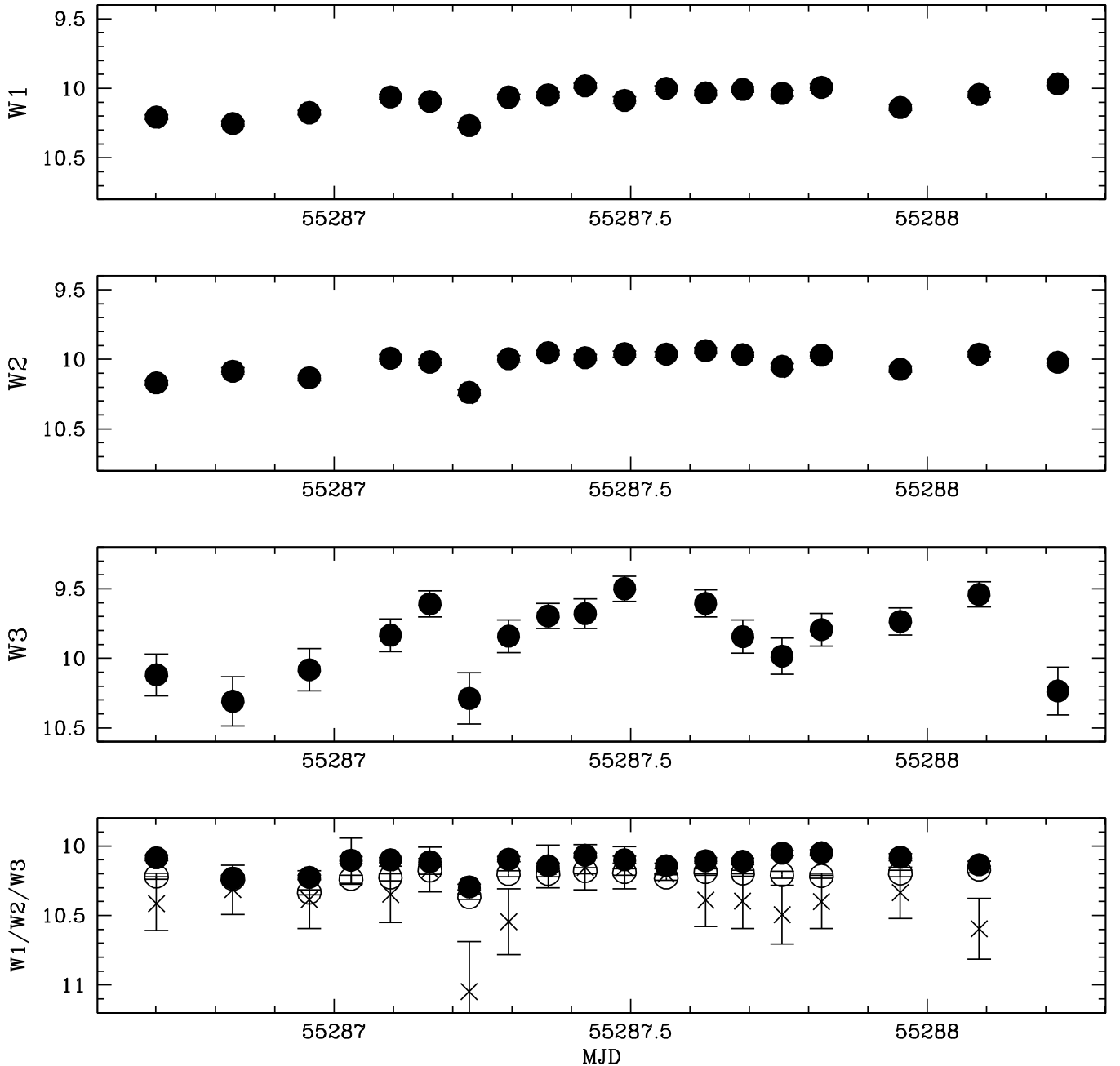


Figure 1. Top three panels present the *WISE* light curves of Z Cam, while the bottom panel presents the data sets for all three *WISE* bandpasses of the nearby field star J082423.40+730628.9. The y-axis for each panel spans an identical magnitude range to fully demonstrate the dramatic variability of Z Cam in the *W3* bandpass.

Table 1
WISE Magnitudes for Z Cam

W1	W2	W3	W4
10.23 ± 0.02	10.17 ± 0.02	9.67 ± 0.05	≥ 8.4

To compare the *WISE* outburst spectral energy distribution (SED) with that at quiescence, we have extracted archival *Spitzer* data for Z Cam. The source was observed with IRAC (Fazio et al. 2004) on MJD53663, using the Infrared Spectrograph peak-up array (Houck et al. 2004) on MJD53654, and with MIPS (Rieke et al. 2004) on MJD53687. The fluxes for the *Spitzer* observations were derived using MOPEX (Makovoz et al. 2006), and are listed in Table 2. The AAVSO data base

shows that Z Cam was in quiescence on all three dates, with a visual magnitude of 12.7, though it went into outburst shortly after the MIPS observation. We present the high (stars) and low state (filled circles) SEDs of Z Cam in Figure 2 with the addition of maximum light optical photometry from Warner (1976) and minimum light optical data from Bruch & Engel (1994). Quiescent *JHK* data is from the Two Micron All Sky Survey.

Harrison & Gehrz (1992) originally reported a weak *IRAS* $12\ \mu\text{m}$ detection of Z Cam ($S_v = 0.09 \pm 0.03$ Jy). A re-examination of the *IRAS* detections for classical novae using *WISE* imaging data (Harrison et al. 2013) showed that the majority of those detections were due to source confusion. This explanation cannot be used to dismiss the detection of Z Cam, as no *WISE* sources this bright exist within the *IRAS*

Table 2
Spitzer Data for Z Cam

3.6 μm (mJy)	4.5 μm (mJy)	5.8 μm (mJy)	8.0 μm (mJy)	15.8 μm (mJy)	24 μm (mJy)
16.41 ± 0.07	11.40 ± 0.06	7.99 ± 0.13	4.74 ± 0.07	1.18 ± 0.04	0.76 ± 0.01

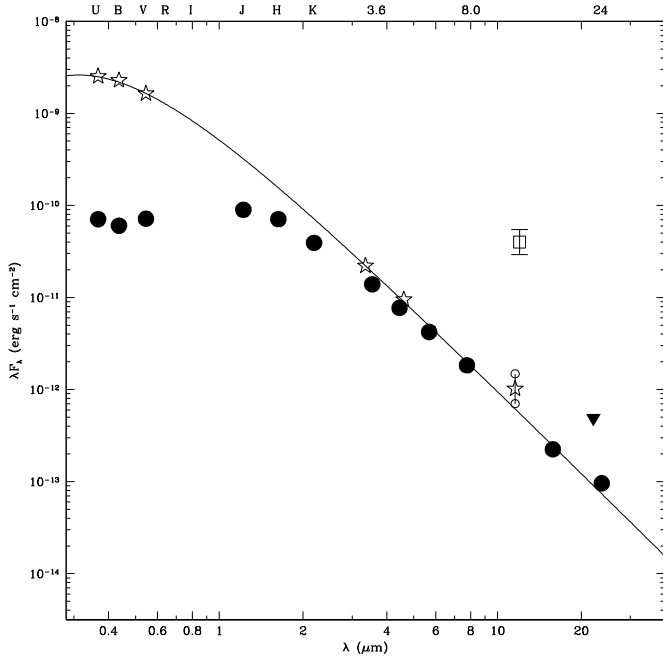


Figure 2. SED of Z Cam in outburst (stars) and in quiescence (filled circles). The solid line is a 15,000 K blackbody normalized to the maximum light *V*-band flux. For the *WISE* W3 data point, we have indicated the range in brightness exhibited in this bandpass by the two small open circles that are connected by a short line segment. The *IRAS* 12 μm flux is indicated by the open square, and the *WISE* W4 limit by the triangle.

detection radius for this source. We have used the “Scanpi” software on the IRSA Web site for *IRAS* data analysis to re-investigate the reported detection of Z Cam. There were 13 unique 12 μm detector scans that crossed the position of Z Cam on four different observational epochs. Co-addition of all of these scans does not result in a detection of Z Cam at signal-to-noise ratio (S/N) ≥ 3 . Fortuitously, however, six of these scans occurred on 1983 April 15, when Z Cam was at visual maximum. Co-addition of the four lowest noise detector scans on this date results in a detection of Z Cam with a flux density of $S_\nu = 0.16 \pm 0.05$ Jy. While this is a very weak detection and therefore somewhat suspicious, co-addition of the data on any of the other three observational epochs does not produce a detection. For these other dates, Z Cam was in quiescence.

3. DISCUSSION

The *WISE* observations of Z Cam began on 2010 March 31.7, and ran to 2010 April 2.2. The AAVSO light curve shows that Z Cam rose from $v \sim 11.5$ to 10.7 over the course of the *WISE* observations. The peak of the outburst ($v \sim 10.6$) occurred near 2010 April 2.8. Both the *W1* and *W2* light curves are consistent with a slow rise of about 0.3 mag over the duration of the observations. As demonstrated by SS Cyg (Harrison et al. 2010), the change in brightness in the near/mid-IR from minimum to maximum in CVs is much smaller than seen at optical wavelengths.

What is striking about the *WISE* observations is the *W3* light curve. It shows large scale variability over the duration of the data set. The total amplitude is 0.8 mag. Phasing the *W3* light curve to the orbital period (6.956 hr) does not reveal a correlation of the variations with phase. The lack of similar sized variations at shorter wavelengths points to only one logical emission source: a synchrotron jet. While thermal emission from cool dust can be used to explain a long wavelength excess (e.g., Hoard et al. 2014), there is no realistic mechanism to create 0.8 mag variations on the hours timescale using dust. Free-free emission in a strong wind could be highly variable, but should exhibit co-temporal variations at shorter wavelengths, while also causing the underlying SED to strongly deviate from a blackbody. Assuming a spherical bremsstrahlung wind source with a spectrum of the form of $f_\nu \propto \nu^{0.6}$ (Wright & Barlow 1975), and the underlying, observed, high state SED as the baseline from which any variability could occur, we would expect 0.8 mag variations in *W3* to lead to coordinated 0.3 mag variations in *W2*. Such variations are not observed.

It is also difficult to have a free-free wind source with this luminosity *and* for it to vary on short timescales. Dubus et al. (2004) explicitly explore this scenario in reference to their mid-IR observations of SS Cyg, an object that also varied by a factor of two on short timescales. They found that the mass loss rate needed in a wind to explain the observed flux was higher than the accretion rate of the underlying binary. Such a source would also have to be as large, or larger than, the binary, and such an object could not undergo large changes on short timescales. A similar result, $1.5 \times 10^{-9} M_\odot \text{ yr}^{-1}$, is attained for Z Cam.

Synchrotron emission has the properties necessary to explain the behavior of Z Cam. In the optically thin regime, it has a spectral slope that declines to higher frequency, allowing long wavelength variability that is not mirrored at shorter wavelengths, and synchrotron sources are highly variable. There are two applicable synchrotron emission processes to consider, the expanding blob/propeller model as in AE Aqr, or a compact jet source. Both lead to similar spectra, an optically thin portion at high frequencies that has a negative slope, $\alpha < 0$ (where $f_\nu \propto \nu^\alpha$), and a flat, or inverted spectral index ($\alpha \geq 0$) at low frequencies (cf. Hjellming & Johnston 1988).

The large amplitude variations of Z Cam in the *W3* bandpass are similar in scale to the radio (Bastian et al. 1988) and mid-IR (Dubus et al. 2004) variations seen in AE Aqr. As discussed in both papers, to simultaneously maintain both the mid-IR and radio variability and the flat radio spectrum, requires the superposition of the emission from a large number of blobs of various sizes. The *W3* light curve of Z Cam has too poor of a temporal resolution to directly compare it to the radio light curves of AE Aqr. Z Cam, however, is not a magnetic CV, and thus it is unclear whether the magnetic propeller blob acceleration mechanism used to explain the behavior of AE Aqr is valid here.

Körding et al. (2008) conclude that the radio observations of SS Cyg are most consistent with a jet. They propose that it had a compact radio jet during the initial rise to outburst, followed by an ejection event to create the peak in the light curve, and

then the restarting of the compact jet in the decline phase. This scenario follows the outline developed to explain the behavior of the jet emission in X-ray binaries as detailed in Fender et al. (2004). The SED of Z Cam in outburst and quiescence shown in Figure 2 suggests that the observed minima in the $W3$ bandpass light curve are very close to the hot blackbody that we have fit to the UBV , and $W1/W2$ fluxes. This would argue that the synchrotron source was essentially not present at the beginning and end of the period spanned by the $WISE$ light curves. The $W3$ light curve is also consistent with having three separate peaks in the light curve that had amplitudes that were about 40% of the total 0.8 mag variability. Similar-sized flares have been observed in the X-ray binary jet sources GX 17+2 and GRS 1915+105 (see Harrison et al. 2014 and references therein).

It is quite interesting that the longest wavelength ($24\ \mu\text{m}$) MIPS data point during quiescence has a flux that is slightly above the extrapolation of the outburst blackbody model. As noted earlier, the MIPS observation occurred very close to the onset of an outburst. Perhaps some synchrotron emission can be generated even before the system has gone fully into outburst. Alternatively, Z Cam produces a small amount of free-free emission at all phases in its outburst cycle. We have also plotted the $12\ \mu\text{m}$ *IRAS* detection in Figure 2. If this is indeed a real measurement of the synchrotron emission of Z Cam, it is much higher relative to the outburst continuum ($60\times$) than that seen in the *IRAS* detection of SS Cyg ($4\times$; see Harrison et al. 2010).

Hoard et al. (2014) presented mid-IR data for a sample of nova-like variables, systems with high mass accretion rates. Several of those systems appeared to have significant mid-IR excesses. Hoard et al. preferred to explain those excesses as due to circumbinary dust emission. cursory examination of the $WISE$ light curves for a number of their sources, however, shows rapid variability in the mid-IR. Using the arguments above leads us to conclude that some of those objects might be sources of synchrotron emission.

4. CONCLUSIONS

The highly variable $12\ \mu\text{m}$ light curve of Z Cam during an outburst suggests that, like SS Cyg, it is a synchrotron source when near visual maximum. If so, it would join the small family of synchrotron emitting CVs: SS Cyg, AE Aqr, V1223 Sgr (Harrison et al. 2010), and probably EX Hya (Harrison et al. 2010) and GK Per (Harrison et al. 2013). There is a significant number of non-magnetic CVs in the AllWISE survey catalog that have extreme ($W2 - W3$) colors that suggest that they too are sources of non-thermal emission. If the *IRAS* detection of Z Cam is in fact real, then it exceeded the observed brightness of SS Cyg at that wavelength. Radio observations of Z Cam are clearly warranted, as would be a large survey of CVs given the sensitivity of the EVLA compared to what was used in previous radio surveys (e.g., Cordova et al. 1983). While we have previously dismissed the *IRAS* detections of CVs as resulting from source confusion, it now appears a worthwhile project to re-examine any reported detection of those sources to see if

they were observed during outburst given that sensitive $12\ \mu\text{m}$ images of their fields now exist.

As discussed by Casse (2008), the standard picture for the collimation of a jet by an accretion disk invokes a magnetohydrodynamic turbulence that generates a twisted poloidal field which acts to collimate the outflow. The result is that some of the angular momentum in the disk is transferred into the production of the collimating magnetic field and the subsequent acceleration of the outflowing material that comprises the jet. These ingredients have not been incorporated into the standard DIM that attempts to explain the outbursts of CVs. Thus, the continued failure of the DIM model to fully explain the eruptions of dwarf novae (e.g., Cannizzo et al. 2010) might partially be related to the ignorance of magnetic field processes in their disks. Note that an additional source of angular momentum loss, beyond that supplied by magnetic braking in the secondary star's wind (Verbunt & Zwaan 1981), would be a welcome addition to our understanding of how CVs operate (cf. Andronov et al. 2003). A full characterization of the jets that are spawned by CVs, and the types of CVs that are capable of launching such jets, would supply dramatic new insight into the physics of their accretion disks.

REFERENCES

- Andronov, I. L., Pinsonneault, M., & Sills, A. 2003, *ApJ*, 582, 358
 Bastian, T. S., Dulk, G. A., & Channugam, G. 1988, *ApJ*, 324, 431
 Bruch, A., & Engel, A. 1994, *A&AS*, 104, 79
 Cannizzo, J. K., Still, M. D., Howell, S. B., Wood, M. A., & Smale, A. P. 2010, *ApJ*, 725, 1393
 Casse, F. 2008, *PPCF*, 50, 1
 Cordova, F. A., Mason, K. O., & Hjellming, R. M. 1983, *PASP*, 95, 69
 Dubus, G., Campbell, R., Kern, B., Taam, R. E., & Spruit, H. C. 2004, *MNRAS*, 349, 869
 Fazio, G. G., Hora, J. L., Allen, L. E., et al. 2004, *ApJS*, 154, 10
 Fender, R. P., Belloni, T. M., & Gallo, E. 2004, *MNRAS*, 355, 1105
 Harrison, T., & Gehrz, R. D. 1992, *AJ*, 103, 243
 Harrison, T. E., Bornak, J., Rupen, M. P., & Howell, S. B. 2010, *ApJ*, 710, 325
 Harrison, T. E., Campbell, R. D., & Lyke, J. E. 2013, *AJ*, 146, 37
 Harrison, T. E., Gelino, D. M., Buxton, M. M., & Fost, T. 2014, *AJ*, 148, 22
 Hjellming, R. M., & Johnston, K. J. 1988, *ApJ*, 328, 600
 Hoard, D. W., Long, K. S., Howell, S. B., et al. 2014, *ApJ*, 786, 68
 Honeycutt, R. K., Robertson, J. W., Turner, G. W., & Mattei, J. A. 1998, *PASP*, 110, 676
 Houck, J. R., Roellig, T. L., Van Cleve, J., et al. 2004, *Proc. SPIE*, 5487, 62
 Jameson, R. F., King, A. R., Bode, M. F., & Evans, A. 1987, *Obs*, 107, 72
 Jarrett, T. H., Cohen, M., Masci, F., et al. 2011, *ApJ*, 735, 112
 K rding, E., Rupen, M., Knigge, C., et al. 2008, *Sci*, 320, 1318
 Livio, M. 1999, *PhR*, 311, 225
 Makovoz, D., Roby, T., Khan, I., & Booth, H. 2006, *Proc. SPIE*, 6274, 10
 Rieke, G. H., Young, E. T., Cadien, J., et al. 2004, *Proc. SPIE*, 5487, 50
 Shafter, A. W., Cannizzo, J. K., & Waagen, E. O. 2005, *PASP*, 117, 931
 Simonsen, M., Boyd, D., Goff, B., et al. 2014, *JAVSO*, 42, 177
 Soker, N., & Lasota, J.-P. 2004, *A&A*, 422, 1039
 Verbunt, F., & Zwaan, C. 1981, *A&A*, 100, 7
 Warner, B. 1976, *Obs*, 96, 49
 Warner, B. 1995, *Cataclysmic Variable Stars* (Cambridge: Cambridge Univ. Press)
 Wright, A. E., & Barlow, M. J. 1975, *MNRAS*, 170, 41
 Wright, E. L., Eisenhardt, P. R. M., Mainzer, A. K., et al. 2010, *AJ*, 140, 1868